Drought in Late Spring of South China in Recent Decades

XIAOGE XIN

State Key Laboratory of Numerical Modeling for Atmospheric Sciences and Geophysical Fluid Dynamics, Institute of Atmospheric Physics, and Graduate School of the Chinese Academy of Sciences, Beijing, China

RUCONG YU

State Key Laboratory of Numerical Modeling for Atmospheric Sciences and Geophysical Fluid Dynamics, Institute of Atmospheric Physics, Chinese Academy of Sciences, and China Meteorological Administration, Beijing, China

TIANJUN ZHOU

State Key Laboratory of Numerical Modeling for Atmospheric Sciences and Geophysical Fluid Dynamics, Institute of Atmospheric Physics, Chinese Academy of Sciences, Beijing, China

BIN WANG

Department of Meteorology, and IPRC, University of Hawaii at Manoa, Honolulu, Hawaii, and State Laboratory of Numerical Modeling for Atmospheric Sciences and Geophysical Fluid Dynamics, Institute of Atmospheric Physics, Chinese Academy of Sciences, Beijing, China

(Manuscript received 8 July 2005, in final form 1 November 2005)

ABSTRACT

Late spring (21 April–20 May) precipitation to the south of the Yangtze River in China along the East Asian front is a salient feature of the global climate. The present analysis reveals that during 1958–2000 South China (26°–31°N, 110°–122°E) has undergone a significant decrease in late spring precipitation since the late 1970s. The sudden reduction of the precipitation concurs with a notable cooling in the upper troposphere over the central China (30°–40°N, 95°–125°E). The upper-level cooling is associated with an anomalous meridional cell with descending motions in the latitudes 26°–35°N and low-level northerly winds over southeastern China (22°–30°N, 110°–125°E), causing deficient rainfall over South China.

The late spring cooling in the upper troposphere over the central China is found to strongly link to the North Atlantic Oscillation (NAO) in the preceding winter. During winters with a positive NAO index, the upper-tropospheric cooling occurs first to the north of the Tibetan Plateau in early–middle spring, then propagates southeastward to central China in late spring. It is suggested that the interdecadal change of the winter NAO is the root cause for the late spring drought over South China in recent decades.

1. Introduction

There have been many studies devoted to the interdecadal changes of the summer precipitation in China, which is characterized by more floods in the Yangtze River Valley and more droughts in North China (e.g., Nitta and Hu 1996; Weng et al. 1999). The cause for the summer rainfall change has attracted much discussion; yet it remains a controversial issue. Some studies attributed it to the increased heating in the tropical Pacific and the tropical Indian Ocean (Chang et al. 2000; Gong and Ho 2002; Hu et al. 2003; Yang and Lau 2004). Menon et al. (2002) suggested that the interdecadal change of the summer rainfall might be induced by the increased release of black carbon aerosols in East Asia. On the other hand, Yu et al. (2004) proposed that the decrease of temperature in the upper troposphere over East Asia plays an essential role in explaining the interdecadal changes in Chinese summer rainfall.

The precipitation band along the East Asian front in April and May, which extends from South China to the

Corresponding author address: Dr. Rucong Yu, LASG, Institute of Atmospheric Physics, Chinese Academy of Sciences, Beijing 100029, China.
E-mail: yrc@lasg.iap.ac.cn

mid–North Pacific, stands out as a salient feature in the global precipitation distribution (Wang et al. 2000). It has been noticed that the spring rainfall in South China also shows obvious changes. There are notable drought trends to south of the Yangtze River in the last 50 years (Hu et al. 2003; Yang and Lau 2004; Zhai et al. 2005). However, the mechanism for the spring drought in China has been discussed little and remains to be elucidated. This study addresses the atmospheric circulation changes associated with the drought and reveal its dynamic processes. Before the analysis, we examined the interdecadal changes (1981–2000 minus 1958–77) of Chinese rainfall from March to May with the pentad mean station precipitation data and found that the South China rainfall decreases mainly from 21 April to 20 May (Julian pentad 23 to 28). This happens to be one month prior to the climatological mean onset date of the East Asian summer monsoon, which is around 20 May, following the monsoon onset over the South China Sea (Wang and LinHo 2002). This study will specifically focus on the rainfall change during the period of 21 April–20 May, which is referred to as late spring (LS). We will show that the interdecadal change of the LS rainfall is concurrent with a cooling in the upper troposphere (500–200 hPa) over central China (30°–40°N, 110°–125°E). The possible cause for this interdecadal rainfall change is discussed in relation to the upper-level cooling. In addition, we explore the possible origin of the upper-tropospheric cooling in an attempt to identify the potential root cause for the rainfall changes in late spring.

The North Atlantic Oscillation (NAO) is one of the major atmospheric teleconnection patterns. Its climate effects across the eastern United States and Western Europe have long been recognized (e.g., Walker and Bliss 1932; van Loon and Rogers 1978; Rogers and van Loon 1979; Rogers 1984; Hurrell 1995; Thompson and Wallace 2001). Recently, the downstream influence of the NAO on the climate in East Asia has also been noticed (Gong et al. 2001; Liu and Yin 2001; Thompson and Wallace 2001; Gong and Ho 2003; Watanabe 2004; Yu and Zhou 2004; Li et al. 2005). This study pays specific attention to exploring the potential linkage between the interdecadal changes of the winter NAO and the LS upper-tropospheric temperature in East Asia.

The paper continues with a description of the data used in this study. The interdecadal variability of the LS rainfall in South China is described in section 3. Section 4 investigates the interdecadal changes of the atmospheric circulation in East Asia and elaborates on the mechanism connecting the South China drought with the upper-tropospheric cooling. Section 5 explores linkages between the central China upper-tropospheric cooling in late spring and the NAO in the preceding winter. The summary is presented in section 6.

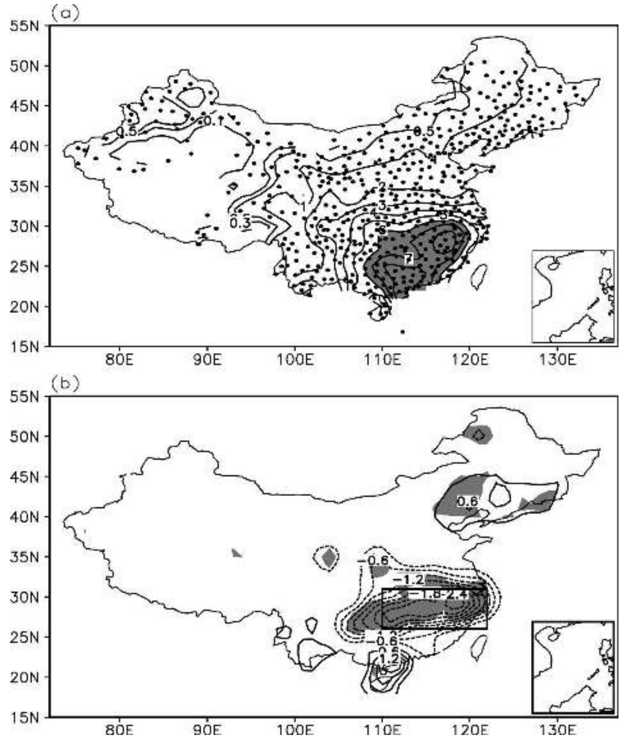

FIG. 1. Climatological mean late spring (21 April–20 May) rainfall in China during (a) 1958–2000, and (b) interdecadal changes (1981–2000 minus 1958–77) of the LS rainfall. Dots in (a) denote the station locations of the precipitation dataset. Shaded regions in (a) represent the rainfall value larger than 6 mm day^{-1}. Shaded regions in (b) represent where the changes of the rainfall are significant at the 5% level.

2. Data

The station precipitation dataset used in this study covers 523 stations in China (locations are shown by dots in Fig. 1a), provided by the Climate Data Center of National Meteorological Information Center, China Meteorological Administration. Almost all station data are available for the period of 1958–2000. The atmospheric circulation data are from the 40-yr reanalysis data of the European Centre for Medium-Range Weather Forecasts (ERA-40; available online at http://data.ecmwf.int/data/d/era40_daily/). The NAO indices of Hurrell (1995) are used in this study. In addition, we use the monthly mean global precipitation dataset Precipitation Reconstruction (PREC; Chen et al. 2002, 2003) as a complementary dataset for examining the rainfall changes in the ocean and checking the results derived from the station precipitation data.

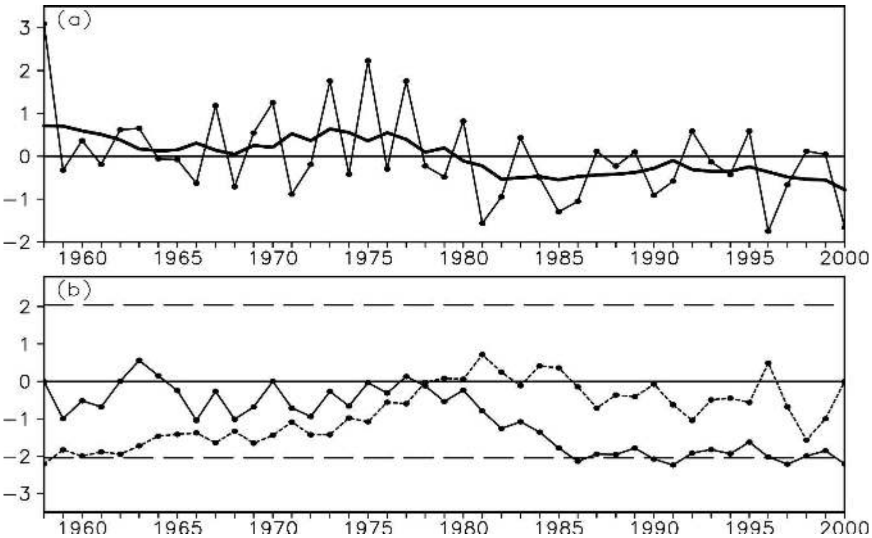

FIG. 2. (a) Normalized time series of the LS SCRI (dotted line) obtained by averaging the rainfall over South China (26°–31°N, 110°–122°E). The thick line represents the 9-yr running mean of the SCRI. (b) The forward (solid dotted line) and backward statistic rank series (dashed dotted line) in the Mann–Kendall test of the SCRI. The dashed beeline indicates the 5% significant level of the Mann–Kendall test.

3. Interdecadal variability of LS rainfall in China

In late spring, the Chinese rainfall is distributed mainly to the south of Yangtze River with the maximum exceeding 8 mm day^{-1} (Fig. 1a). The distribution of the rainfall exhibits a gradual decrease from south (>6 mm day^{-1}) to north (<2 mm day^{-1}) downstream of the Tibetan Plateau. Figure 1b shows the interdecadal change of the LS rainfall, which is denoted by the mean during 1981–2000 minus that during 1958–77. The decrease of the rainfall is remarkable over South China. Increases of the rainfall are distributed along the southern coast of China and in parts of northeastern China. In the following analysis, we will focus our attention on the noticeable drought that occurred in South China.

To measure the variability of rainfall in the drought region, we define normalized time series of the regional mean precipitation over (26°–31°N, 110°–122°E: outlined rectangle in Fig. 1b) from 1958 to 2000 as the South China rainfall index (SCRI). As indicated by the SCRI shown in Fig. 2a, it is rather wet in South China before 1980, especially in the 1970s; while it is extremely dry in the 1980s and 1990s. An interdecadal shift for the South China rainfall can be seen from the low-frequency variation of the SCRI (thick line in Fig. 2a), which shows an obvious high-to-low transition in the late 1970s. To confirm the statistical significance of this sudden change, the Mann–Kendall test (Mann 1945; Kendall 1975) is performed on the SCRI. The two statistic rank series of the test are displayed in Fig. 2b, which cross at the year 1978 within the 5% significant level, so the South China rainfall has likely experienced an interdecadal shift in the late 1970s. Thus, using the difference of the South China rainfall between the two periods of 1981–2000 and 1958–1977 is appropriate for denoting its interdecadal change (Fig. 1b).

4. Atmospheric circulation changes accounting for the South China drought

In this section, we use the difference of the atmospheric circulation between the two periods, 1981–2000 and 1958–77, to explore the circulation changes associated with the interdecadal change of LS rainfall in South China.

a. Circulation changes in the troposphere

As shown in Fig. 3a, in LS southwesterly winds prevail over South China in the lower troposphere, where the wind upstream of the India–Burma trough converges with the southwesterly along the northwestern flank of the western Pacific subtropical high. This airflow provides the major water vapor for the precipitation in South China (Fig. 1a), which is transported mainly from the Bay of Bengal and the South China Sea.

The interdecadal changes of the horizontal winds and

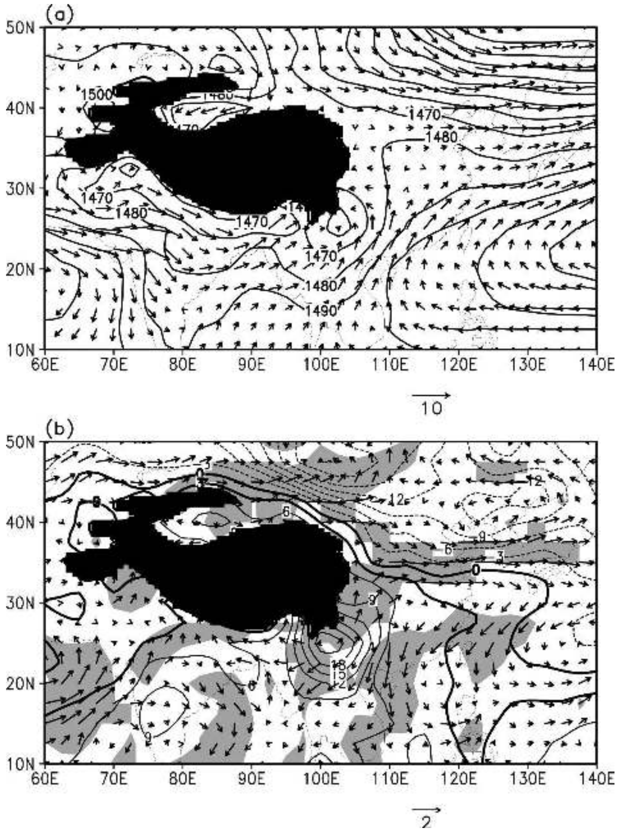

FIG. 3. (a) Climatological mean LS horizontal winds and geopotential height at 850 hPa for 1958–2000. (b) Interdecadal changes (1981–2000 minus 1958–77) of the LS horizontal winds and geopotential height at 850 hPa. The black shaded area in (a) and (b) denote the location of the Tibetan Plateau. The gray shaded regions in (b) represent where the changes of the horizontal winds (u and v) are significant at the 10% level. Units of the wind vectors are m s^{-1}. Units of the geopotential height are gpm.

geopotential height at 850 hPa in LS are shown in Fig. 3b. As indicated by the positive changes in the geopotential height (contour), an anomalous anticyclone appears to the south of 35°N in China. There are anomalous northeasterlies east of the anticyclone, which tend to decrease the water vapor transported to South China and thus lead to less rainfall over South China. In addition, there are cyclonic anomalies in northeast China where the anomalous winds favor for more rainfall there (Fig. 1b).

Prominent atmospheric changes also occur in the upper troposphere. As shown in Fig. 4, the air temperature at 300 hPa decreases significantly over East Asia. The most significant cooling is found over central China, where the temperature is lowered more than 1.0°C. An anomalous cyclone is observed above the cooling region (Fig. 4). This is in agreement with what is expected from the thermal wind relationship.

b. The roles of the central China upper-tropospheric cooling

The above analysis shows that there are distinct interdecadal changes for the atmospheric circulation in the lower and upper troposphere. In this subsection, we will discuss the linkage between these changes and their effects on the South China rainfall.

The zonal–height cross section of the interdecadal changes in the LS temperature (shaded) and geopotential height (contour) along 110°–125°E are shown in Fig. 5a. It can be seen that there is an obvious cooling center over 30°–40°N in the upper troposphere (500–200 hPa). Corresponding to this upper-level cooling, the atmospheric thickness is thinned in the upper troposphere. Thus the geopotential height lowers in the upper troposphere. Underneath the upper-level cooling, the geopotential height rises in the latitudes 22°–32°N. This can be explained by the thermal wind relation in terms of the hydrostatic balance. Accompanied with the upper-level cooling, there are cyclonic anomalies in the upper troposphere and anticyclonic anomalies in the lower troposphere.

Associated with the vorticity anomalies, there are anomalous southerlies in the upper troposphere and northerlies in the lower troposphere over East China (to the east of 110°E: Fig. 5b). The cold dense air in the upper troposphere tends to subside (Fig. 5b). Thus, the anomalous airflows in the upper troposphere and in the lower troposphere together with the anomalous vertical motion constitute a vertical meridional circulation in East China. The subsidence in the latitudes 26°–35°N suppresses convective activity. The anomalous low-level northerlies reduce the water vapor being transported to South China. Thus the existence of the anomalous meridional cell plays a decisive role in decreasing rainfall over South China. The ascending branch of the meridional cell is shown to be in the latitudes 15°–20°N, which might be driven by changes in the divergence field, indicating more rainfall there.

It has been shown qualitatively that the LS upper-tropospheric cooling over central China is associated with prominent changes in the atmospheric circulation, which further cause the drought in South China. To verify this idea, we need to display the variability of the upper-level temperature and circulation variables, which change distinctly, and show their relationship with the SCRI on the interdecadal scale. Based on the above analysis, three indices are defined: The mean temperature in the upper troposphere (500–200 hPa) over central eastern China (30°–40°N, 110°–125°E) during 1958–2000 is defined as the upper-tropospheric temperature index (UTTI) after being normalized. The

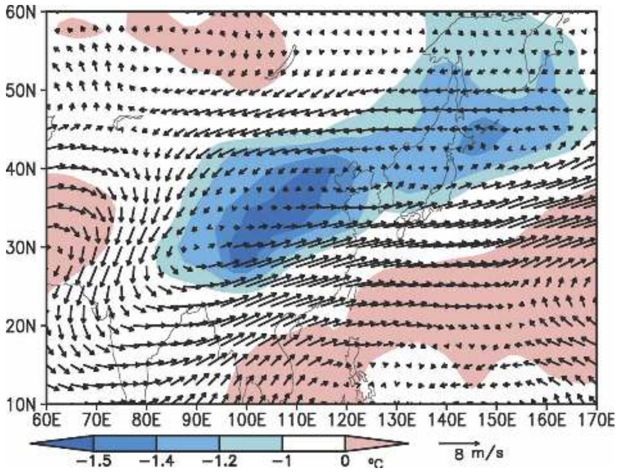

FIG. 4. Interdecadal changes (1981–2000 minus 1958–77) of the LS 300-hPa temperature (shaded, units: °C) and 200-hPa horizontal winds (vectors, units: m s^{-1}).

lower-tropospheric meridional wind index (LTVI) denotes the normalized mean meridional wind velocity over southeastern China (22°–30°N, 110°–125°E) in the lower troposphere (925–850 hPa). The middle tropospheric vertical wind index (MTWI) represents the normalized mean vertical velocity ($-\omega$) over (26°–35°N, 110°–125°E) at 500 hPa. Figure 6 shows that the UTTI was in its high phase in most years before 1978, while it stayed at the low phase in most years after 1978. Such features can also be found in the time series of LTVI and MTWI.

The statistical significance of the interdecadal changes (1981–2000 minus 1958–77) for the three variables; namely, upper-tropospheric temperature, lower-tropospheric meridional wind, and the middle-tropospheric vertical wind are further tested and shown in Table 1. The changes of the upper-tropospheric temperature and the middle-tropospheric vertical velocity both exceed the 1% significance level. The lower-tropospheric northerly changes above the 10% significancet level, which is not as significant as the other two variables. This may be due to fact that external factors for the changes of the low-level circulation are more complicated than that in the middle and upper troposphere.

So the cooling in the upper troposphere, the descending anomaly in the middle troposphere, and the weakening of the southerly flow in low-tropospheric levels occur simultaneously in the late 1970s. This interdecadal transition in the late 1970s for the circulation variables is distinct from the transition years of the three producing streams of the ERA-40 dataset, which are "pre-satellite" during 1957–72, "assimilating some satellite types" during 1972–1988, and "assimilating the

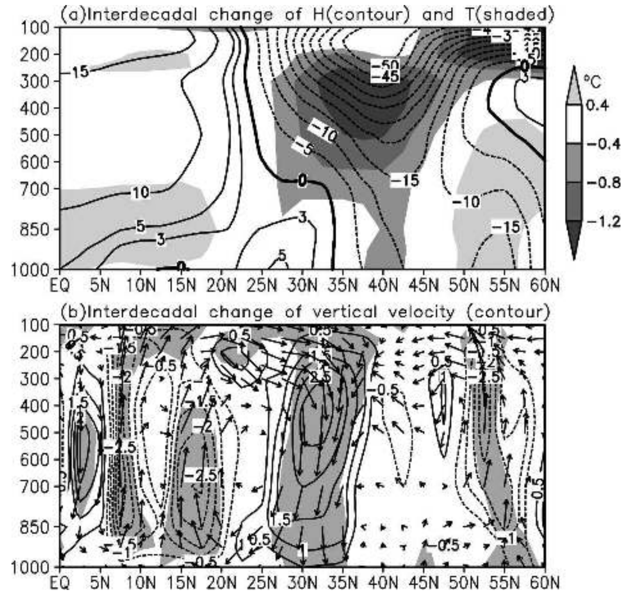

FIG. 5. Zonal–height cross sections of the (a) interdecadal changes (1981–2000 minus 1958–77) in the LS geopotential height (contour, units: gpm) and temperature (shaded, units: °C), and (b) vertical velocity (ω, contour interval 1×10^{-2} hPa s^{-1}) along 110°–125°E. Change of meridional wind (v) and vertical velocity ($-\omega$) are plotted as vectors in (b). Shaded regions in (b) represent where the changes of the vertical velocity are significant at the 5% level.

latest observation types" during 1987–2002 (information available online at http://tornado.badc.rl.ac.uk/data/ecmwf-e40/e40_background.html).

It should be noted that such interdecadal changes of the upper-level temperature and the atmospheric circulation over East Asia are also obvious using National Centers for Environmental Prediction–National Center for Atmospheric Research (NCEP–NCAR) reanalysis data (Kalnay et al. 1996) and the Chinese station radiosonde data (figures not shown).

From Table 1, we can also see the interannual correlation coefficients of the LIVI and MTWI with the UTTI are 0.52 and 0.53, respectively, highly above the 1% significance level. This proves that the changes in the lower tropospheric meridional wind and the middle tropospheric vertical motion are tightly connected with the upper tropospheric cooling. On the other hand, the LWVI and MTWI are both closely correlated with the SCRI, with the significant coefficients of 0.59 and 0.77 (Table 1). This indicates that the weakened southerly flow in the lower troposphere and the anomalous descending motion in the middle troposphere are both important factors for the drought over South China in recent decades. Therefore, the South China drought is connected with the upper-level cooling through the corresponding changes in the atmospheric circulation. This

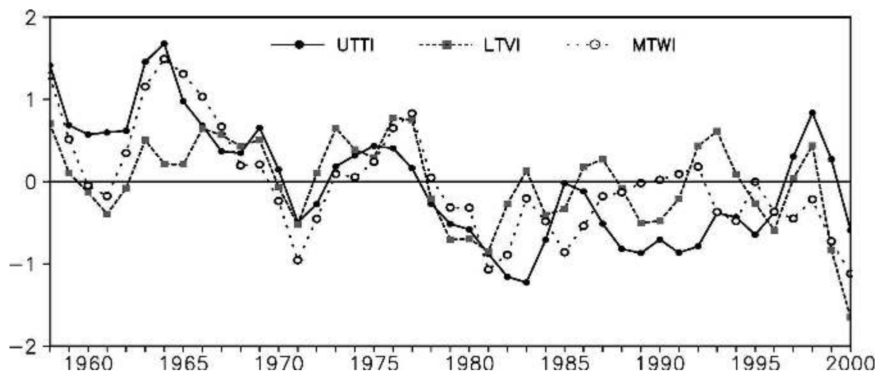

FIG. 6. Time series of 9-yr running mean of the UTTI, LTVI, and MTVI in LS. The UTTI is defined by the normalized mean temperature over (30°–40°N, 110°–125°E) in the upper troposphere (500–200 hPa). The LTVI is defined by the normalized mean meridional wind velocity over (22°–30°N, 110°–125°E) in the lower troposphere (925–850 hPa). The MTWI is defined by the normalized mean vertical wind velocity ($-\omega$) over (26°–31°N, 110°–125°E) in the middle troposphere (500 hPa).

is also validated by the significant correlation between UTTI and SCRI shown in Table 1.

c. *Comparison of the upper-level cooling and rainfall changes between late spring and summer*

From above, the South China drought in LS is closely linked to the upper-tropospheric cooling over central China on the interdecadal scale. Similarly, prominent upper-tropospheric cooling occurs in summer, which accounts for the rainfall-change pattern of the southern flood and northern drought in China (Yu et al. 2004). It is necessary to make clear the differences between late spring and summer about the upper-level cooling and the rainfall changes. Here the monthly global precipitation dataset PREC (Chen et al. 2002, 2003) is used in that the rainfall changes over the ocean need to be displayed. The rainfall in May is chosen to replace that in late spring (21 April–20 May) since a shorter-scale (pentad mean) global precipitation dataset covering the most recent 50 years is not available currently.

Figure 7 shows the interdecadal changes in the upper-tropospheric (500–200 hPa) temperature and rainfall in May and summer. It is clear that the upper-level cooling in May is farther south to that in summer. In May, the cooling is in the latitudes 30°–40°N over East China, while in summer it is in the latitudes 35°–45°N. However, the rainfall changes in the two seasons show a similar feature: the drought is bordered on the southeastern part of the upper-level cooling region. As shown in Fig. 7, the May drought occurs in South China, while the summer drought appears in North China. It is noticed that the drought in May shown here is consistent with that derived from the station precipitation data (figure not shown), and also agrees with the drought in late spring shown in Fig. 1b.

The summer rainfall change exhibits more floods in the Yangtze River valley, comprising a pattern of southern flood and northern drought with the North China drought (Fig. 7b). This is partly attributed to the weakening of the East Asian summer monsoon associated with the upper-tropospheric cooling (Yu et al. 2004). Accordingly, in May the wetness is distributed over the southeastern coast of China, the South China

TABLE 1. Changes of temperature, meridional wind, and vertical velocity, and their correlation coefficients with the UTTI and SCRI during the period of 1958–2000.

	$T_{(500\text{–}200\ \text{hPa})}$ (°C) (30°–40°N, 110°–125°E)	$V_{925\text{–}850\ \text{hPa}}$ (m s^{-1}) (22°–30°N, 110°–125°E)	$-\omega_{500\ \text{hPa}}$ (hpa s^{-1}) (26°–35°N, 110°–125°E)
Change (1981–2000 minus 1958–77)	−1.1**	−0.6*	-2.0×10^{-2}**
Correlation coefficient with UTTI	1.0**	0.52**	0.53**
Correlation coefficient with SCRI	0.45**	0.59**	0.77**

* Significant at the 10% level.
** Significant at the 1% level.

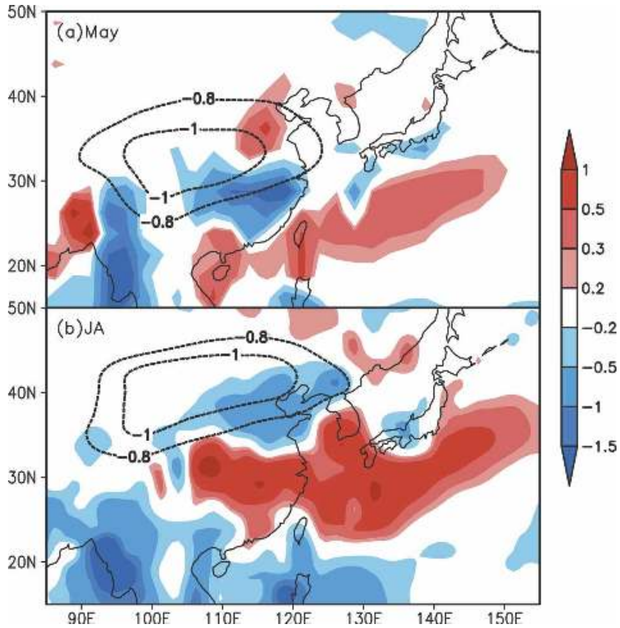

FIG. 7. Interdecadal changes (1981–2000 minus 1958–77) in the upper tropospheric (500–200 hPa) temperature (contour) and the rainfall (shaded) in (a) May, and in (b) summer (July–August; JA). The contour in (a), (b) represents the changes of the temperature lower than $-0.8°C$. The unit of the rainfall is mm day^{-1}.

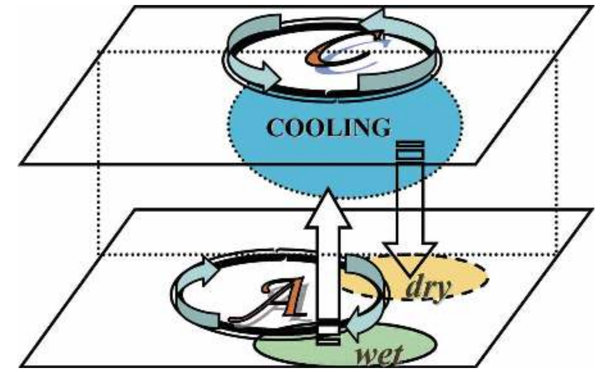

FIG. 8. Schematic diagram showing the effect of the upper-tropospheric cooling on the atmospheric circulation and the precipitation. The arrows denote the anomalous winds. The dashed (solid) circle in the lower layer represents the region of the dry (wet). The letter "C" in the upper layer denotes cyclone, and the letter "A" in the lower layer denotes anticyclone.

Sea, and the northwestern Pacific (Fig. 7a). In a certain sense, the rainfall changes in May also exhibit a pattern of southern flood and northern drought. It is noticed that the "flood" region covers the island of Taiwan, indicating where the May rainfall increases after the late 1970s. This is in agreement with the result obtained from the station observational data in Taiwan (Hung et al. 2004).

The similarity in the rainfall change pattern in May and summer validates the essential effects of the upper-tropospheric cooling on the surface climate condition. On the basis of the above study and the study of Yu et al. (2004), we draw a schematic diagram showing the relationship between the upper-tropospheric cooling and the rainfall changes in China (Fig. 8). When the atmosphere is cooled in the upper troposphere, there are cyclonic anomalies in the upper troposphere and anticyclonic anomalies in the lower troposphere. The anomalous upper-level southerlies and low-level northerlies exist in the eastern part of the cooling region. Meanwhile, anomalous descending motion prevails beneath the cooling region because of the increased airmass extent. Ascending motions appear to the south of the cooling region where the divergence field changes because of the airflow anomalies in the upper troposphere and lower troposphere. Thus an anomalous meridional circulation forms. The downward branch and the low-level branch of the meridional cell suppress the rainfall bordered on the southeastern part of the cooling region. The weakened southwesterly in China implies the southward retreat of the rainband. So the rainfall increases to the south of the drought region. This is also the region where the anomalous ascending motion prevails. Therefore, the rainfall changes associated with the upper-tropospheric cooling show a pattern of southern flood and northern drought.

5. Linkages between the central China upper-tropospheric cooling in LS and the NAO in the preceding winter

Due to the important roles of the upper-tropospheric cooling in the rainfall changes over East Asia, causes of the cooling should be clarified. Yu et al. (2004) showed that the summer upper-tropospheric cooling links to the lower-stratospheric cooling significantly. However, such a relationship cannot be found in late spring. Some studies showed that the early spring temperature change in East Asia is related to the preceding winter NAO (Yu and Zhou 2004; Li et al. 2005). In this section, we will explore possible connections between the winter NAO and the late spring upper-tropospheric temperature in East Asia.

The normalized time series of the winter (January–March: JFM) NAO index and the LS UTTI are shown in Fig. 9a. It can be seen that the LS UTTI varies inversely correlated with the winter NAO index. The correlation coefficient between them is -0.59, above the 1% significance level. This suggests that the NAO in the preceding winter is a significant predictor for the LS

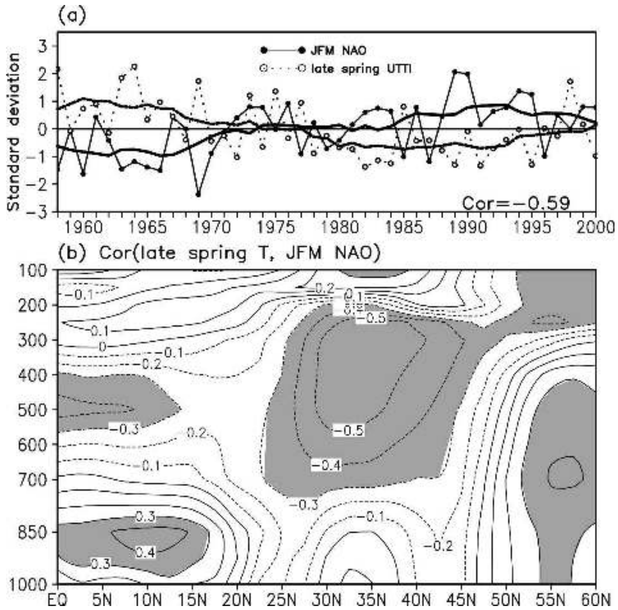

FIG. 9. (a) Normalized time series of the winter (JFM) NAO index (solid line with filled circle) and the LS UTTI (dashed line with open circle). The solid (dashed) thick line represents the 9-yr running mean of the winter NAO (LS UTTI). (b) Zonal–height distributions of the correlation coefficients between the winter NAO index and the LS air temperature along 110°–125°E. Shaded regions in (b) are significant at the 5% level.

upper-troposphere temperature over central China. The out-of-phase variation between the two indices is shown to be not only on the interannual scale but also on the interdecadal scale. This implies that the abrupt decrease of the LS upper-tropospheric temperature over central China may result from the unprecedented strongly positive winter NAO index after the late 1970s.

The relationship between the winter NAO and the LS upper-tropospheric temperature over East Asia is further revealed in Fig. 9b, which shows the zonal–height distribution of the correlation coefficients between the winter NAO and the LS temperature along 110°–125°E. The negative correlation is shown to be prominent in the upper troposphere over central China. This correlation map bears a striking spatial resemblance to the interdecadal change of the LS temperature (Fig. 5a), which testifies the possible influence of the winter NAO on the LS upper-tropospheric temperature in East Asia on the interdecadal scale.

It was noticed that the winter NAO-related cooling resides in the lower troposphere in March, and it exists in the upper troposphere in April (Figs. 4c,d in Yu and Zhou 2004). In fact, from April to May the cooling signal in the upper troposphere related to the winter NAO migrates. In early–middle April, the upper-level cooling is centered north of the Tibetan Plateau (Fig. 10a). Then the cooling signal propagates southeastward to central-eastern China in LS (Fig. 10b). In late May, the cooling signal weakens and moves to northeast China (Fig. 10c). It is the strong cooling signal in LS that associates with remarkable changes in the atmospheric circulation over East Asia that result in the South China drought. However, the mechanism involved in the movement of the winter NAO-related cooling from April to May is still unclear and needs further investigations.

6. Summary

The South China (26°–31°N, 110°–122°E) rainfall in late spring has decreased significantly since the late 1970s. This is derived from not only the station observational precipitation data in China, but also the global monthly mean precipitation dataset PREC. Such changes of rainfall occur concurrently with a cooling in the upper troposphere (500–200 hPa) over central China (30°–40°N, 95°–125°E). The dynamic processes linking the South China drought to the upper-level

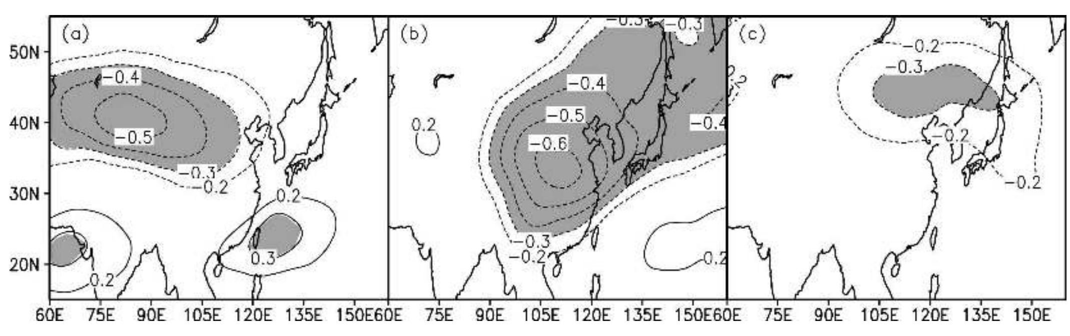

FIG. 10. Distributions of the correlation coefficients between the winter (JFM) NAO index and the mean air temperature in the upper troposphere (500–200 hPa) during (a) 1–20 April, (b) 21 April–20 May (LS), and (c) 21–31 May from 1958 to 2000. Shaded regions are significant at the 5% level.

cooling are then explored. Results show that the upper-tropospheric cooling is associated with cyclonic anomalies in the upper troposphere, anticyclonic anomalies in the lower troposphere, and anomalous descending motion beneath the upper cooling region. Thus, an anomalous meridional circulation cell exists over East China. Both the downward branch and the low-level branch of the meridional cell play important roles in decreasing the rainfall over South China. Meanwhile, the meridional circulation anomaly leads to more rainfall over the southeastern coast of China, the South China Sea, and the northwestern Pacific, constituting a pattern of southern flood and northern drought. This pattern appears to the south of that in summer because of the corresponding differences in the location of the cooling region in the two seasons.

The possible causes of the upper-tropospheric cooling in late spring over central China are further investigated. It is found that this late spring upper-level cooling is closely connected with the interdecadal change of the preceding winter (JFM) NAO index. The central China upper-level temperature in late spring decreased significantly after the late 1970s, when the preceding winter NAO shifted to its highly positive phase. During April–May, the upper-level cooling signal related to the positive winter NAO is not stationary. The cooling appears to the north of Tibetan Plateau in early–middle April. It then moves southeastward and resides over central China in late spring. This phenomenon raises the possibility that the interdecadal change of NAO in winter could have decreased the South China rainfall in the following late spring.

Acknowledgments. This work was jointly supported by the Chinese Academy of Sciences through the International Partnership Creative Group called The Climate System Model Development and Application Studies, the Knowledge Innovation Program (KZCX3-SW-221), and by the National Natural Science Foundation of China under Grants 40233031 and 40375029.

REFERENCES

Chang, C.-P., Y. S. Zhang, and T. Li, 2000: Interannual and interdecadal variations of the East Asian summer monsoon and tropical Pacific SSTs. Part II: Meridional structure of the monsoon. *J. Climate,* **13,** 4326–4340.

Chen, M., P. Xie, J. E. Janowiak, and P. A. Arkin, 2002: Global land precipitation: A 50-yr monthly analysis based on gauge observations. *J. Hydrometeor.,* **3,** 249–266.

——, ——, ——, ——, and T. M. Smith, 2003: Reconstruction of the oceanic precipitation from 1948 to the present. Preprints, *14th Symp. on Global Changes and Climate Variations,* Long Beach, CA, Amer. Meteor. Soc., CD-ROM, 3.5.

Gong, D.-Y., and C.-H. Ho, 2002: Shift in the summer rainfall over the Yangtze River valley in the late 1970s. *Geophys. Res. Lett.,* **29,** 1436, doi:10.1029/2001GL014523.

——, and ——, 2003: Arctic Oscillation signals in the East Asian summer monsoon. *J. Geophys. Res.,* **108,** 4066, doi:10.1029/2002JD002193.

——, S. W. Wang, and J. H. Zhu, 2001: East Asian winter monsoon and Arctic Oscillation. *Geophys. Res. Lett.,* **28,** 2073–2076.

Hu, Z.-Z., S. Yang, and R.-G. Wu, 2003: Long-term climate variations in China and global warming signals. *J. Geophys. Res.,* **108,** 4614, doi:10.1029/2003JD003651.

Hung, C.-W., H.-H. Hsu, and M.-M. Lu, 2004: Decadal oscillation of spring rain in northern Taiwan. *Geophys. Res. Lett.,* **31,** L22206, doi:10.1029/2004GL021344.

Hurrell, J. W., 1995: Decadal trends in the North Atlantic Oscillation: Regional temperatures and precipitation. *Science,* **269,** 676–679.

Kalnay, E., and Coauthors, 1996: The NCEP/NCAR 40-Year Reanalysis Project. *Bull. Amer. Meteor. Soc.,* **77,** 437–471.

Kendall, M. G., 1975: *Rank Correlation Measures*. Charles Griffin, London, 202 pp.

Li, J., R. C. Yu, T. J. Zhou, and B. Wang, 2005: Why is there an early spring cooling shift downstream of the Tibetan Plateau? *J. Climate,* **18,** 4660–4668.

Liu, X. D., and Z.-Y. Yin, 2001: Spatial and temporal variation of summer precipitation over the eastern Tibetan Plateau and the North Atlantic Oscillation. *J. Climate,* **14,** 2896–2909.

Mann, H. B., 1945: Nonparametric tests against trend. *Econometrica,* **13,** 245–259.

Menon, S., J. Hansen, L. Nazarenko, and Y. Luo, 2002: Climate effects of black carbon aerosols in China and India. *Science,* **297,** 2250–2253.

Nitta, T., and Z.-Z. Hu, 1996: Summer climate variability in China and its association with 500-hPa height and tropical convection. *J. Meteor. Soc. Japan,* **74,** 425–445.

Rogers, J. C., 1984: Association between the North Atlantic Oscillation and the Southern Oscillation in the Northern Hemisphere. *Mon. Wea. Rev.,* **112,** 1999–2015.

——, and H. van Loon, 1979: The seesaw in winter temperatures between Greenland and northern Europe. Part II: Some oceanic and atmospheric effects in middle and high latitudes. *Mon. Wea. Rev.,* **107,** 509–519.

Thompson, D. W. J., and J. M. Wallace, 2001: Regional climate impacts of the Northern Hemisphere annular mode. *Science,* **293,** 85–89.

van Loon, H., and J. C. Rogers, 1978: Seesaw in winter temperatures between Greenland and northern Europe. Part I: General description. *Mon. Wea. Rev.,* **106,** 296–310.

Walker, G. T., and E. W. Bliss, 1932: World weather V. *Mem. Roy. Meteor. Soc.,* **4,** 53–84.

Wang, B., and LinHo, 2002: Rainy seasons of the Asian–Pacific summer monsoon. *J. Climate,* **15,** 386–398.

——, R. Wu, and X. Fu, 2000: Pacific–East Asia teleconnection: How does ENSO affect East Asian climate? *J. Climate,* **13,** 1517–1536.

Watanabe, M., 2004: Asian jet waveguide and a downstream extension of the North Atlantic Oscillation. *J. Climate,* **17,** 4674–4691.

Weng, H.-Y., K.-M. Lau, and Y.-K. Xue, 1999: Multi-scale summer rainfall variability over China and its long-term link to global sea surface temperature variability. *J. Meteor. Soc. Japan,* **77,** 845–857.

Yang, F. L., and K.-M. Lau, 2004: Trend and variability of China precipitation in spring and summer. *Int. J. Climatol.,* **24,** 1625–1644.

Yu, R.-C., and T.-J. Zhou, 2004: Impacts of winter-NAO on March cooling trends over subtropical Eurasia continent in the recent half century. *Geophys. Res. Lett.,* **31,** L12204, doi:10.1029/2004GL019814.

——, B. Wang, and T.-J. Zhou, 2004: Tropospheric cooling and summer monsoon weakening trend over East Asia. *Geophys. Res. Lett.,* **31,** L22212, doi:10.1029/2004GL021270.

Zhai, P. M., X. B. Zhang, H. Wan, and X. H. Pan, 2005: Trends in total precipitation and frequency of daily precipitation extremes over China. *J. Climate,* **18,** 1096–1108.